Synthesis and characterization of pure and combined cobalt and titanium oxides nanoparticles for dye removal applications

Z. A. Jasim *, J. A. Abd

University of Babylon, College of Science for Women, Department of Laser Physics, Hilla-Najaf Street, Babylon, 51002, Iraq

In this study we present the detail of synthesis and characterization of (Co₃O₄) and (TiO₂) nanoparticles as well as their composites as (Co₃O₄@Tio₂) and (Tio₂@Co₃O₄). These particles were prepared in deionized water by using pulsed laser ablation method with an Nd-YAG laser of 4 nsec duration and 1064 nm wavelength. The produced nanoparticles were comprehensively characterized by implementing FE-SEM, XRD, and FTIR investigations. In general, the prepared nanoparticles possess spherical or semispherical shapes with cubic crystal phase of (Co₃O₄) and tetragonal phase of the (TiO₂). The characteristics of the nanoparticles indicate their importance in a large number of applications including photo-catalytic.

(Received June, 12, 2025; Accepted September 4, 2025)

Keywords: Co₃O₄, TiO₂, Co₃O₄@TiO₂, TiO₂@Co₃O₄, Pulsed laser ablation

1. Introduction

Quantum size effects and the large surface area enable important and unique properties in the nano-size materials that are significantly different than those of bulk materials [1-3]. This has made this kind of material the focus of great number of studies. Cobalt oxide (Co₃O₄) is one of the important materials that have been employed in a large number of critical electrochemical, photochemical, and photonics applications [4,5]. This pushes the experts in the field of material science to produce Co₃O₄ nanostructures in form of particles, hollow spheres, rods, plates, wires, tubes, and cubes. In addition, the porosity of Co₃O₄ nanostructures have been tuned to enhance their functional properties in various applications [6,7].

Titanium dioxide is a low cost and easy-to-use material. It has higher chemical stability compared to other catalysts. TiO₂ is widely used in photoelectronic devices mainly due to its wide band gap [8]. In addition, it is widely used in water purification applications as an efficient photocatalyst [9, 10]. In particular, the anatase and rutile crystalline forms of TiO₂ are the most widely used phases in the photo-catalytic applications due to the high photo-activity of the anatase form and the high thermodynamic stability of the rutile crystalline form [11, 12]. Important results have been achieved in the field of photo-catalyst by using TiO2 nanostructures [9, 10]. However, there are few studies about the surface characterization of the brookite crystalline form of TiO₂.

In this work, we introduce a comprehensive characterization of cobalt oxide and titanium oxide nanoparticles as well as their composition as core@shell structures synthesized by pulsed laser ablation technique. Field Emission Scanning Electron Microscope (FE-SEM) examination was used to investigate the shape and the size distribution of the prepared nanoparticles. X-ray diffraction (XRD) examination and Fourier Transform Infrared spectroscopy (FTIR) were used to examine the crystalline state and the composition of the prepared nanostructures, respectively.

2. Experimental part

The nanoparticles studied in this work were synthesized by using pulsed laser ablation in liquid (PLAL) technique. PLAL includes several basic steps. First, two separate targets, one of

^{*} Corresponding author: scw147.zainab.asid@student.uobabylon.edu.iq https://doi.org/10.15251/DJNB.2025.203.1005

(Co₃O₄) and the other of (TiO₂), were made by mechanically compressing solid (Co₃O₄ and TiO₂) micro scale-powders. A constant pressure of (30 MPa) was applied, resulting in compact discs of suitable density for use as solid targets in laser ablation process.

Second, a disk of (Co_3O_4) was immersed into deionized water to prepare nanoparticles of (Co_3O_4) . A 300 mJ Nd-YAG laser at 1064 nm wavelength and pulse duration of (4 nsec) was used. Different number of laser pulses was used (500,750, and 1000 pulses) to prepare different concentrations of the nanoparticles. The same process was used to prepare TiO_2 nanoparticles but with a different number of laser pulses (100,200, and 300 pulses).

For preparing $(Co_3O_4@TiO_2)$, first, the same process of creating the Co_3O_4 was followed. After that, the (Co_3O_4) disk was replaced by the (TiO_2) disk to create (TiO_2) nanoparticles under the same laser conditions. The $(Co_3O_4@TiO_2)$ sample was prepared using 500 pulses for (Co_3O_4) and 200 pulses for (TiO_2) . The $(TiO_2@Co_3O_4)$ sample was prepared by using 300 pulses for (TiO_2) and 500 pulses for (Co_3O_4) .

The XRD measurements were performed by using a DX2700BH device with silicon drift detector. ΣIGMA, JSM-7610F, Carl Zeiss instrument operating at an accelerating voltage of 10KV was used to perform the FESEM measurements. The FTIR measurements were done by using a BRUKER FTIR spectrometer.

3. Results and discussion

3.1. Field emission-scanning electron microscopy (FE-SEM)

FE-SEM measurements were used to analyze the morphological properties and to determine the dimensions of the nanoparticles produced by PLA process. Figure (1) presents three FE-SEM images for the Co_3O_4 nanoparticles prepared in deionized water by using different numbers of laser pulses (500-750-1000 p).

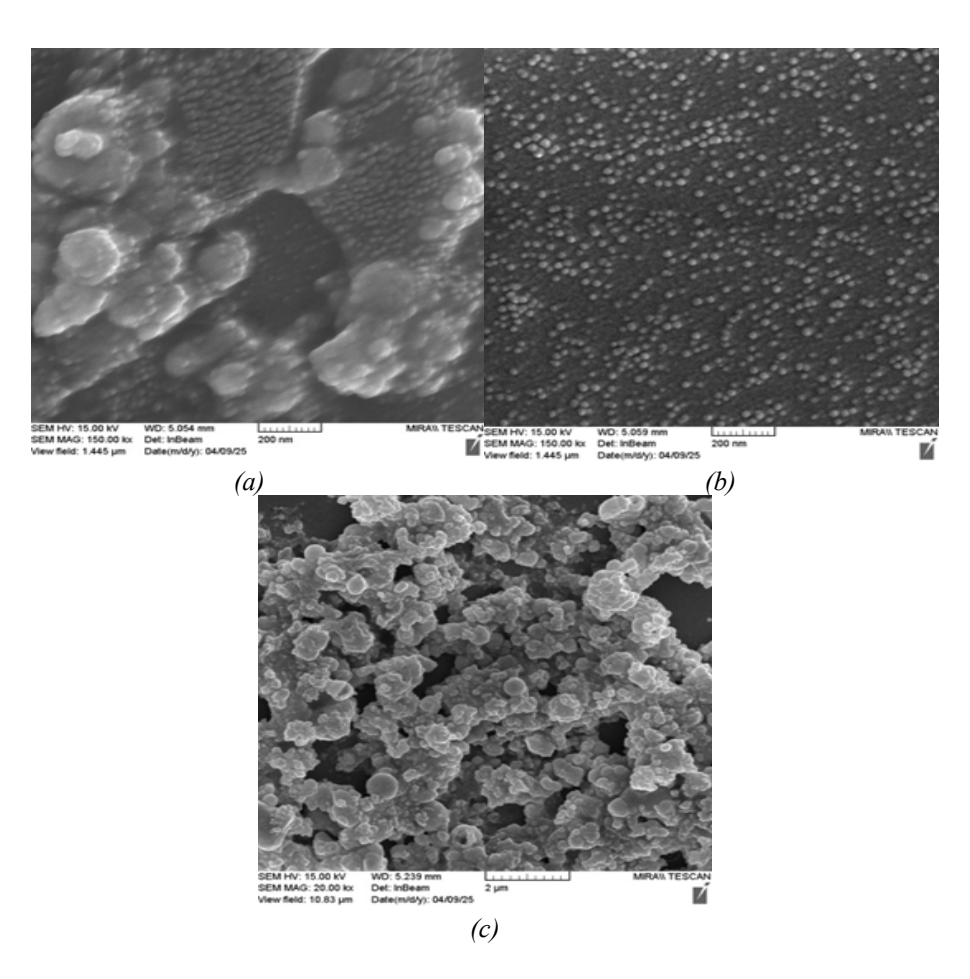


Fig. 1. FE-SEM image of Co_3O_4 nanoparticles prepared by Laser ablation by using (a) 500p (b) 750 p and (c) 1000p.

Figure (1 a) clearly shows that the particles have spherical and semi-spherical shapes with sizes ranging from (20 nm) to (80 nm). These particles clumped together at the stage of preparing the FE-SEM samples. Figure (1b) shows an area of the Co_3O_4 sample where the particles are separated. The particles of this sample are much smaller in size than those prepared with 500 pulses. This could be due to the larger lasers action in the sample or it just an abnormal area of the sample. The second assumption is more likely to be the reason because the particles prepared with 1000 pulses, shown in figure (1 c), exhibit almost the same properties as those shown in figure (1 a). This means that changing the number of pulses does not have a significant influence on the shape and the size of the synthesized particles.

Figure (2 a) shows two FE-SEM images of (TiO₂) nanoparticles prepared with (200) and (300) laser pulses. It is clear the particles have spherical and semispherical shapes but they aggregate together to form irregular shapes. The sizes of the particles range between 50-150 nm. Looking at Figure (2 b) implies that, the number of pulses does not have a significant influence on the shape of the particles. The spherical shape of is a characteristic of most nanoparticles prepared by pulsed laser ablation [13, 14].

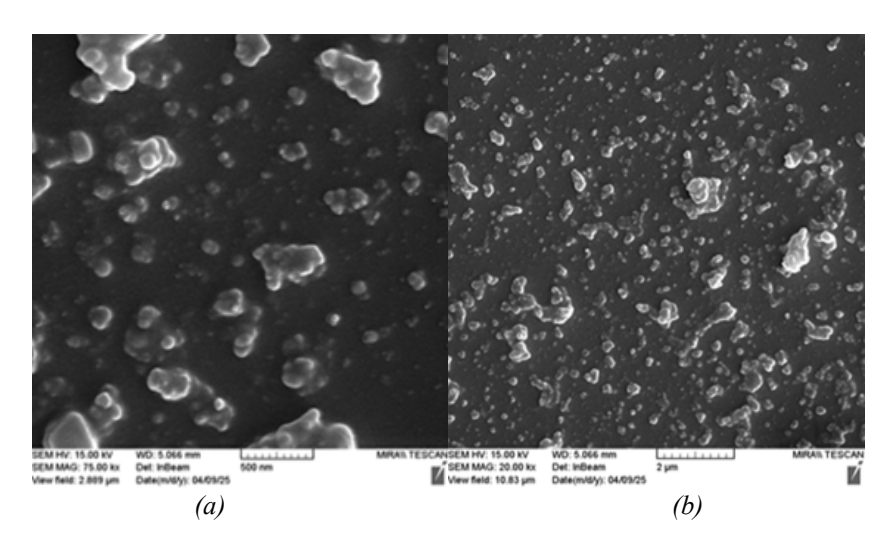
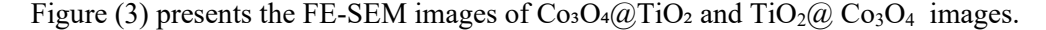


Fig. 2. FE-SEM image of TiO_2 nanoparticles prepared by laser ablation with (a) 200 pulses and (b) 300 pulses.



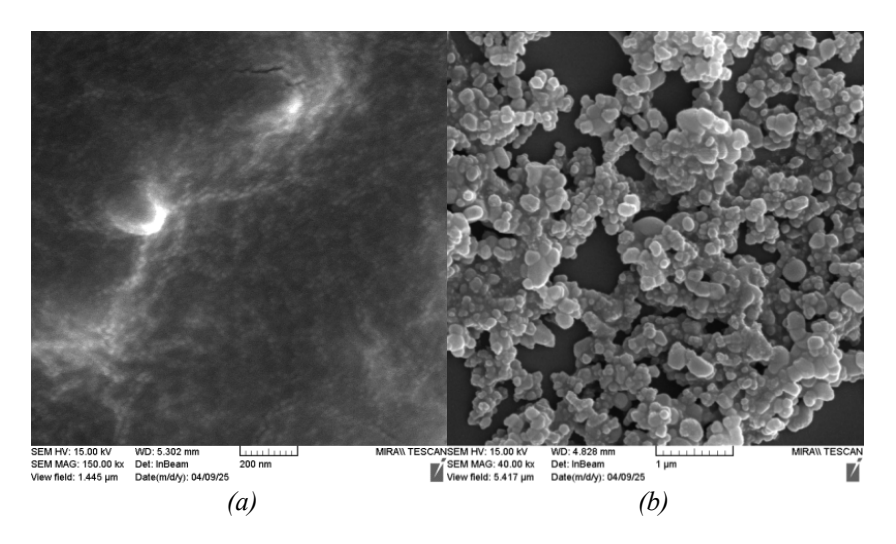


Fig. 3. FE-SEM image of (a) Co_3O_4 @ TiO_2 and (b) TiO_2 @ Co_3O_4 nanoparticles.

The images reveal that some particles exhibit a regular spherical shape, while others are clustered into dense aggregates. The results in this figure indicate that the combination of Co_3O_4 with TiO_2 does not enhance the aggregation properties of the particles.

3.2. FTIR examination results

Figure (4) shows the FTIR spectra of the prepared samples. The spectrum of the Co₃O₄ nanoparticles shows a band at (566cm⁻¹) and a sharp band at (665cm⁻¹) arising from Co-O bond stretching vibrations and the bridging vibration of O-Co-O bond, respectively [13]. They confirm the formation of Co₃O₄ spinel oxide [14]. The intense band at (1636.04cm⁻¹) is attributed to the bending mode of H₂O. The broadband around (3400cm⁻¹) is attributed to the stretching of the bond between hydrogen and oxygen of H₂O molecules [14, 17, 18].

The spectrum of (TiO₂) nanoparticles contains a peak at (594cm⁻¹) corresponds to stretching vibrations of Ti-O and Ti-O-Ti [19]. The peak located at (1639.66 cm⁻¹) corresponds to the H-O-H bending mode bond [20]. The sharp peak at (3417.59 cm⁻¹) is attributed to the stretching vibration of the O-H bond [21].

The figure of $(Co_3O_4@TiO_2)$ shows bands at (675.04, 1636.55, 3384.05, 3852.85, and $3898.62 \text{ cm}^{-1})$. The broad band at 675.04 cm^{-1} is a result of the merger of multiple peaks attributed to Co-O, and Co-O-Co vibrations [15] as well as Ti-O and Ti-O-Ti vibrations [19]. The band at (1636.55cm^{-1}) and (3384cm^{-1}) are associated with water molecules [22]. The result confirms the presence of both Co_3O_4 and TiO_2 material in the composition. The spectrum of the $(Tio_2@Co_3O_4)$ nanoparticles is not noticeably different than that of $(Co_3O_4@TiO_2)$. The absorption bands at the short wavenumbers, below 700 cm^{-1} , belong to the vibrations of the metal oxides [23].

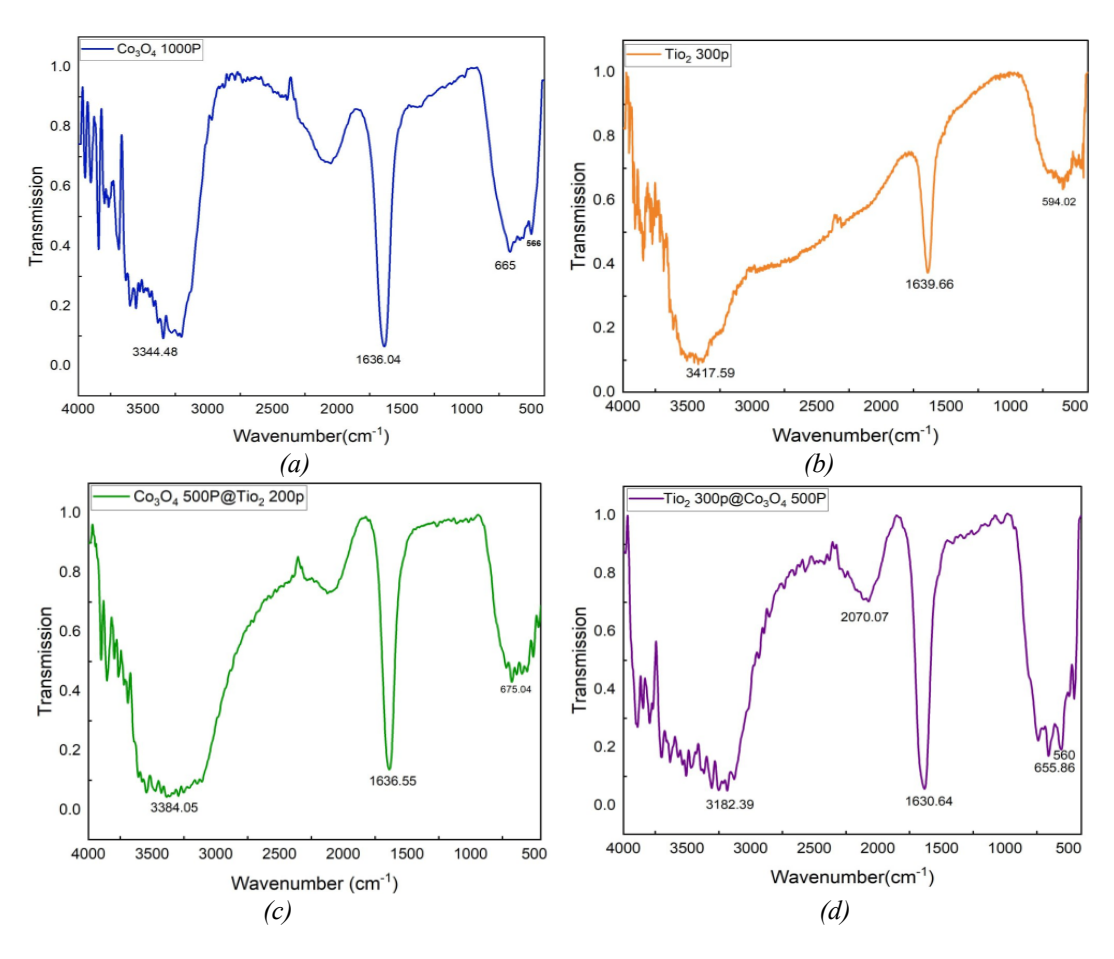


Fig. 4. FTIR spectra of Co₃O₄, TiO₂, Co₃O₄ @TiO₂, and TiO₂@Co₃O₄.

3.3. XRD examination results

Figure (5) shows the X-ray diffraction patterns of the prepared samples.

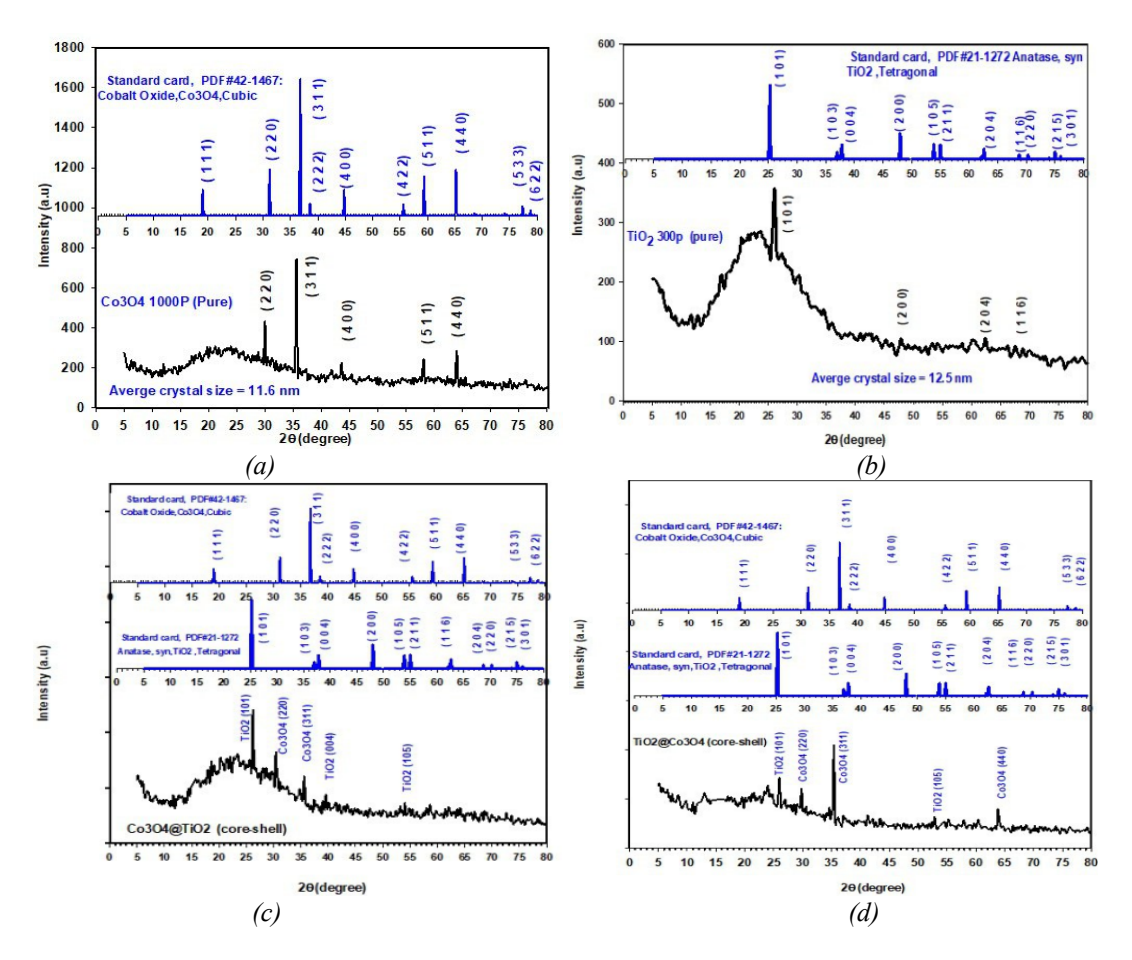


Fig. 5. XRD patterns of (a) (Co_3O_4) (b) TiO_2), (c) Co_3O_4 @ TiO_2 , and (d) TiO_2 @ Co_3O_4 nanoparticles.

Figure (5a) shows sharp and narrow peaks at angle (2θ) of (28.51, 35.65, 43.42, 58.11, and (63.97) which correspond to crystalline planes of (220), (311), (400), (511), and (440), respectively. These results indicate the cubic crystalline nature of the (200) material according to card No. (PDF#42-1467). In addition, the results indicate that no impurities or contaminants were detected in the sample.

X-ray diffraction pattern of titanium dioxide nanoparticles, shown in figure (5b), contains four diffraction peaks appear at 20 of (26.16, 47.76, 63, and 69.82). They correspond to the crystalline planes ([101], [200], [204], and [116]), respectively. These results and the sharp peak at (25.2), which corresponds to the plane [101], reveal the anatase crystalline phase of the titanium dioxide nanoparticles according to card No. (PDF#21-1272) [24].

Figure (5c and 5d) show the X-ray diffraction pattern of (Co₃O₄@TiO₂ and TiO₂@Co₃O₄) nanoparticles. Frame (c) of the figure presents sharp peaks at 2θ of (26.32, 41.38, and 54.46) which correspond to the crystalline planes ([101], [004], and [105]) of the anatase phase of titanium dioxide according to cards (PDF#21-1272). The reduction in the intensity of the two peaks at (41.38, and 54.46) could be due to the coverage of the Co₃O₄ shell. Diffraction peaks at (2θ) of (30.53, and 37.78) belong to crystalline planes of ([220], and [311]) of cubic Co₃O₄ nanoparticles according to card No. (PDF#42-1467). The diffraction pattern in figure (5 d) of (TiO₂@Co₃O₄) contains two peaks at (25.730 and 52.830) which correspond the crystalline planes ([101] and [105]) of the anatase phase of titanium dioxide. The other peaks at (29.64, 37.11, and

63.85) correspond to the planes ([220], [311], and [440]), respectively. They indicate the presence and the cubic structure of the (Co₃O₄) nanoparticles.

4. Conclusion

The preparation and the characterization of (Co_3O_4) , (TiO_2) , $(Co_3O_4@TiO_2)$, and $(TiO_2@Co_3O_4)$ nanoparticles in deionized water was presented. Field Emission-Scanning Electron Microscopy (FE-SEM) images of all prepared samples showed spherical or semispherical shapes forming clusters of different sizes. The presence of the (Co_3O_4) and (TiO_2) material was confirmed by the Fourier transform infrared measurement. The pure (Co_3O_4) and (TiO_2) particles prepared by pulsed laser ablation have cubic and anatase tetragonal crystalline phases, respectively. The integration of the components into a core@shell structure does not affect the crystalline phase of either material.

References

- [1] Klabunde KJ, Richards RM, Nanoscale Materials in Chemistry, 2nd edition. Wiley, New York; 2012.
- [2] H. A. Majeed, H. M. Sobhi, R. M. Baiee, A. B. Sharba, A. Al-Nafiey, Plasmonics, 1 (2024); https://doi.org/10.1007/s11468-024-02604-x.
- [3] H. M. Sobhi, A. B. Sharba, J. M. Jassim, Journal of Nanostructures, **13**(2), 567 (2023; https://doi.org/10.22052/JNS.2023.02.027
- [4] V. R. Mate, M. Shirai, C. V. Rode, Catalysis Communications, **33**(5), 66 (2013); https://doi.org/10.1016/j.catcom.2012.12.015.
- [5] S. A. Makhlouf, Journal of Magnetism and Magnetic Materials, **246**(1-2), 184 (2002); https://doi.org/10.1016/S0304-8853(02)00050-1.
- [6] L. Sun, H. Li, L. Ren, C. Hu, Solid State Sciences **11**(1), 108 (2009); https://doi.org/10.1016/j.solidstatesciences.2008.05.013
- [7] L-X. Yang, Y-J. Zhu, L. Li, L. Zhang, H. Tong, W-W. Wang, G-F. Cheng, J-F. Zhu, European Journal of Inorganic Chemistry, **2006**(23), 4787 (2006); https://doi.org/10.1002/ejic.200600553
- [8] Y. Zhao, C. Li, X. Liu, F. Gu, H. Jiang, W. Shao, L. Zhang, Y. He, Materials Letters **61**(1),79(2007); https://doi.org/10.1016/j.matlet.2006.04.010.
- [9] A. L. Linsebigler, G. Lu, J. T. Yates, Jr, Chemical Reviews, **95**(3),735(1995); https://doi.org/10.1021/cr00035a013
- [10] A Fujishima, T. N. Rao, D. A. Try, Electrochimica Acta, **45**(28), 4683(2000); https://doi.org/10.1016/S0013-4686(00)00620-4
- [11] M. A. Henderson, Surface Science Reports, **66** (6-7),185 (2011); https://doi.org/10.1016/j.surfrep.2011.01.001
- [12] N. T. Nolan, D. W. Synnott, M. K. Seery, S. J. Hinder, A. V. Wassenhoven, S. C. Pillai, Journal of Hazardous Materials, **212**(15), 88 (2012); https://doi.org/10.1016/j.jhazmat.2011.08.074.
- [13] D. Dorranian, E. Solati, L. Dejam, Materials Science & Processing, **109**, 307(2012); https://doi.org/10.1007/s00339-012-7073-5
- [14] A. S. Ahmed, A. B. Sharba, Q. M. Salman, Chalcogenide Letters **21** (12), 989 (2024); https://doi.org/10.15251/CL.2024.2112.989
- [15] H. Xu, Z. Hai, J. Diwu, Q. Zhang, L. Gao, D. Cui, J. Zang, J. Liu, C. Xue, Journal of Nanomaterials, **1953**(1), 8 (2018); https://doi.org/10.1063/1.5032330
- [16] M. Salavati-Niasari, A. Khansari, F. Davar, Inorganica Chimica Acta, **362**(14), 4937 (2008); https://doi.org/10.1016/j.ica.2009.07.023
- [17] A. B. Sharba, R. T. Ahmed, S. F. Haddawi, Journal of Nonlinear Optical Physics & Materials, **31**(04), 2250020 (2022); https://doi.org/10.1142/S0218863522500205.

- [18] D. Zou, C. Xu, H. L. L. Wang, T. Ying, Materials Letters, **62**(12-13), 1976 (2008); https://doi.org/10.1016/j.matlet.2007.10.056
- [19] P. M. Kumar, S. Badrinarayanan, M. Sastry, Thin Solid Films, **358**(1-2), 122 (2000); https://doi.org/10.1016/S0040-6090(99)00722-1
- [20] L. Xiong, C. Chen, Q. Chen, J. Ni, Journal of Hazardous Materials, **189**(3), 741 (2011); https://doi.org/10.1016/j.jhazmat.2011.03.006
- [21] A. Slav, Digest Journal of Nanomaterials and Biostructures 6, 915 (2011).
- [22] M. Zhang, R. Sun, Y. Li, Q. Shi, L. Xie, J. Chen, X. Xu, H. Shi, W. Zhao, The Journal of Physical Chemistry C, **120**(20), 10746 (2016); https://doi.org/10.1021/acs.jpcc.6b01030
- [23] M. Salavati-Niasari, A. Khansari, F. Davar, Inorganica Chimica Acta, **362**(14), 4937 (2009); https://doi.org/10.1016/j.ica.2009.07.023
- [24] A. Hu, X. Zhang, D. Luong, K. D. Oakes, M. R. Servos, R. Liang, S. Kurdi, P. Peng, Y. Zhou, Waste and Biomass Valorization, 3, 433 (2012); https://doi.org/10.1007/s12649-012-9142-6